



OPEN

Intraoperative hyperspectral imaging (HSI) as a new diagnostic tool for the detection of cartilage degeneration

Max Kistler¹, Hannes Köhler², Jan Theopold¹, Ines Gockel³, Andreas Roth¹, Pierre Hepp¹ & Georg Osterhoff[✉]

To investigate, whether hyperspectral imaging (HSI) is able to reliably differentiate between healthy and damaged cartilage tissue. A prospective diagnostic study was performed including 21 patients undergoing open knee surgery. HSI data were acquired during surgery, and the joint surface's cartilage was assessed according to the ICRS cartilage injury score. The HSI system records light spectra from 500 to 1000 nm and generates several parameters including tissue water index (TWI) and the absorbance at 960 nm and 540 nm. Receiver operating characteristic curves were calculated to assess test parameters for threshold values of HSI. Areas with a cartilage defect ICRS grade ≥ 3 showed a significantly lower TWI ($p = 0.026$) and higher values for 540 nm ($p < 0.001$). No difference was seen for 960 nm ($p = 0.244$). For a threshold of 540 nm > 0.74 , a cartilage defect ICRS grade ≥ 3 could be detected with a sensitivity of 0.81 and a specificity of 0.81. TWI was not suitable for cartilage defect detection. HSI can provide reliable parameters to differentiate healthy and damaged cartilage. Our data clearly suggest that the difference in absorbance at 540 nm would be the best parameter to achieve accurate identification of damaged cartilage.

Cartilage degeneration as seen in osteoarthritis is a common disease, causing pain and disability. It frequently results in a need for prolonged non-operative therapy, ultimately surgical joint replacement, causing a relevant socio-economic burden to the individual and the society¹.

Imaging modalities currently used to detect cartilage or joint degeneration are radiography and magnetic resonance imaging (MRI). Radiography can only use surrogate parameters for cartilage degeneration, as the joint space width². Those morphological changes occur at later stages of cartilage degeneration only^{2,3}. While radiography is still the most common and least expensive technique, MRI is able to visualize the cartilage directly and to show biochemical changes, like an increase of water content of the cartilage tissue in the early stages of degeneration²⁻⁴. Still, it remains difficult to precisely image the thin articular cartilage and to detect small fibrillations⁵ and initial degenerative changes⁶.

Another method to examine cartilage is arthroscopy. This invasive procedure is necessary, because sometimes, the above-mentioned imaging modalities alone are not sufficient. There are cases, in which changes in cartilage are seen through direct visualization using arthroscopy. However, MRI and the findings of arthroscopy do not always correlate well⁷⁻⁹. In such cases, the examiner currently has visual scores at his disposal to objectify those lesions only, e.g. the International Cartilage Repair Society (ICRS)-Cartilage Injury Classification¹⁰. Because of this and differences in experience, there is a large inter-observer variance in arthroscopy as well as in MRI^{6,8}. Initial changes are also difficult to detect by arthroscopy⁶, and sometimes there are already degenerative changes in visually healthy cartilage¹¹.

Hyperspectral Imaging (HSI) is a relatively new technique that can show biochemical and morphological information and changes in tissue, even if they are not visible by the surgeon's judgment. The combination of spectroscopy and imaging in one process allows this¹². The advantage of the in vivo spectral imaging is that functional and structural pathologic changes of the tissues can be detected at the same time and be used direct grading of tissue damage without the need of a biopsy¹³. Therefore, it is a valuable tool to detect the changes in

¹Department of Orthopaedics, Trauma and Plastic Surgery, University Hospital Leipzig, 04103 Leipzig, Germany. ²Innovation Center Computer Assisted Surgery (ICCAS), University of Leipzig, Leipzig, Germany. ³Department of Visceral, Transplant, Thoracic and Vascular Surgery, Leipzig University Hospital, Leipzig, Germany. ✉email: georg.osterhoff@medizin.uni-leipzig.de

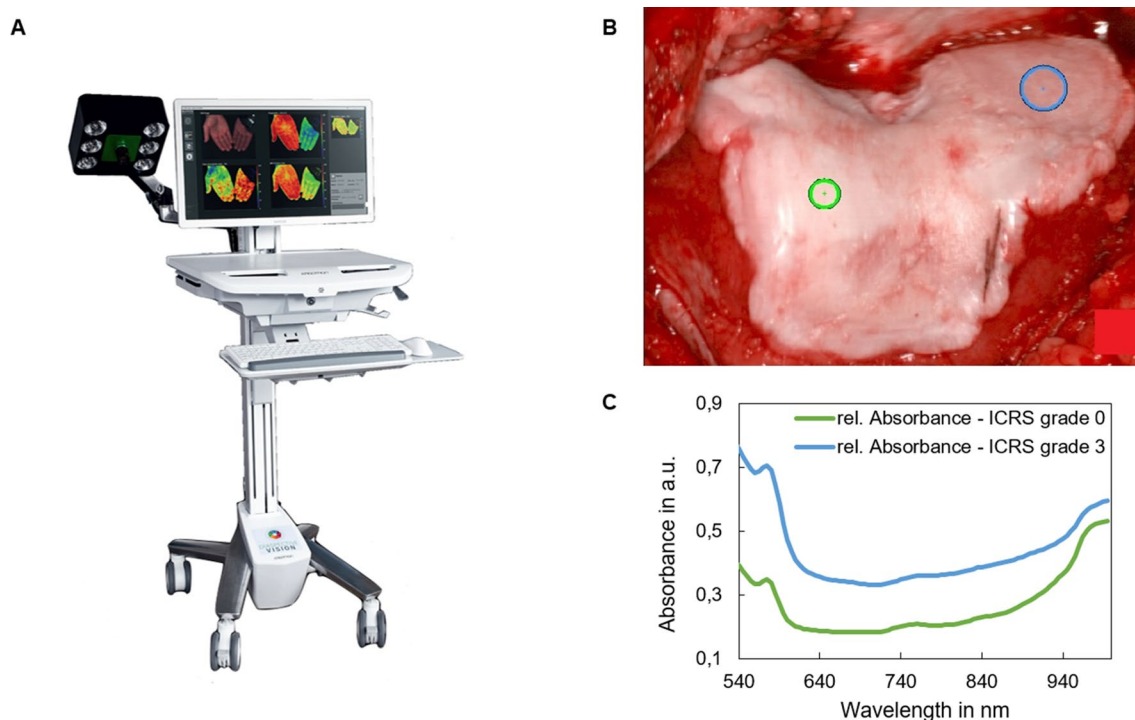


Figure 1. Hyperspectral Imaging-acquisition. **(A)** HSI camera (TIVITA Tissue, image reproduced] from Diaspective Vision GmbH, Germany, all rights reserved). **(B)** RGB image with markers (small green marker: ICRS grade 0, large blue marker: ICRS grade 3). **(C)** Spectral data for cartilage marked ICRS grade 0 and ICRS grade 3. The spectra are calculated as follows: $IR = (I_0 - I_{dark}) / (I_{white} - I_{dark})$, where I_{dark} is the dark pattern without illumination, I_0 is the acquired intensity, and I_{white} is the intensity measured on a white reference. The absorbance A was calculated by $A = -\log_{10}(IR)$.

morphology mentioned above, which occur in degenerated cartilage. It has already been used successfully to detect such changes e.g. in a carcinoma^{14–16} or in ischemic tissue^{17–19}, and it has been applied to differentiate tissues based on their spectral properties^{20,21}.

The current study aims to investigate whether the HSI technique is able to reliably differentiate between healthy and damaged cartilage tissue, and therefore to detect areas of cartilage degeneration.

Patients and methods

Patients. The protocol of this prospective diagnostic study was approved by the ethics committee of the Medical Faculty of the University of Leipzig (reference 393/16-ek). All methods were performed in accordance with the relevant guidelines and regulations. Consecutive patients aged 18 and older, who underwent total or hemiarthroplasty for degenerative osteoarthritis of the knee between March and December 2019 and gave informed consent, were included. In total, 21 patients (19 female) with a median age of 63 years (43 to 84) were included.

Data acquisition. During surgery and before resection of the joint surfaces, images were taken using the Hyperspectral Imaging camera (TIVITA Tissue, Diaspective Vision GmbH, Germany). The system uses a built-in halogen light source to record reflectance spectra from 500 to 1000 nm in 6.4 s. The field of view (FOV) for all parameters was $21 \times 30 \text{ cm}^2$ and the spatial resolution was 0.56 mm at 630 nm (evaluated with the 1951 USAF resolution test chart at 50 cm object distance). A more detailed description of the used HSI camera system has previously been published by Holmer et al.²²

An experienced fellowship-trained surgeon assessed the joint surface and defined areas with a cartilage defect of ≥ 3 according to the International Cartilage Repair Society (ICRS) Cartilage Injury Classification¹⁰, as well as areas with a cartilage defect of $ICRS < 2$, serving as healthy control. These areas were manually labelled on the plain red–green–blue RGB image of the joint surface to allow for comparison during analysis of the HSI data later (Fig. 1).

Using the HSI data, tissue water index (TWI), as well as relative absorbance at 960 nm and at 540 nm were chosen from the near-infrared and visible spectrum as candidate parameters. A wavelength of 960 nm was chosen as in the range of 500 nm to 1000 nm, as the absorption coefficient of water shows its maximum at 960 nm. Our selection of parameters was based on previous studies with animal cadaver cartilage specimens^{23–26} and parameters previously described by Holmer et al.²² In addition, threshold values for the classification of cartilage defects were identified based on the spectra (Fig. 1C).

| | Cartilage | | <i>p</i> |
|--------|-------------|-------------|----------|
| | Healthy | Damaged | |
| TWI | 75 ± 15 | 67 ± 12 | 0.026 |
| 540 nm | 0.59 ± 0.27 | 1.18 ± 0.48 | < 0.001 |
| 960 nm | 0.47 ± 0.10 | 0.49 ± 0.07 | 0.244 |

Table 1. Relative absorbance and TWI of healthy and damaged cartilage.

TIVITA Suite automatically generates false colour images for physiological tissue parameters, calculating indices, e.g. for oxygenation and perfusion, showing the values from 0 to 100 color-coded. The TWI is calculated for the water content with:

$$\text{TWI} = \frac{\frac{\text{mean}(955-980\text{nm})}{\text{mean}(880-900\text{nm})} - s1}{s2 - s1},$$

$s1$, and $s2$ being parameters to scale the values between 0 and 100²².

Statistical analysis. All calculations were performed with TIVITA Suite and SPSS 25.0. Continuous data are presented as mean and standard deviation (SD), categorical data in frequencies and percentages. After testing for normal distribution using the Shapiro–Wilk test, either a paired Student's-t test or paired non-parametric tests were used to detect differences in means between healthy and damaged cartilage. The level of significance was defined as $p < 0.05$.

Receiver operating characteristic (ROC) tables were computed to examine the sensitivity and specificity of threshold values of the HSI parameters that showed significant differences in means and would correctly indicate a cartilage defect. A priori, we decided that a threshold of > 80% sensitivity and specificity represented a clinically acceptable margin of error, as these are in range of a decile of the values achieved by magnetic resonance imaging (sensitivity 0.72–a0.87, specificity 0.86–a0.89)²⁷.

Ethics approval. All methods were performed in accordance with the relevant guidelines and regulations. The protocol of this prospective diagnostic study was approved by the ethics committee of the Medical Faculty of the University of Leipzig (reference 393/16-ek).

Consent to participate and publication. All participants gave informed consent to the use of their data and images for analysis and publication.

Results

ICRS grading. All specimens contained areas of healthy (ICRS grade < 2) and damaged cartilage (ICRS grade ≥ 3). Two of 21 cartilage defects (9.5%) were ICRS grade 4, all others (90.5%) were grade 3.

Hyperspectral imaging. Areas with a cartilage defect ICRS grade ≥ 3 showed a significantly lower TWI ($p = 0.026$, Table 1, Fig. 2), and higher values for 540 nm ($p < 0.001$). No difference was seen for 960 nm ($p = 0.244$).

ROC analysis. As only TWI and 540 nm revealed significant differences in means between healthy and damaged cartilage, ROC tables were computed for these two parameters only. With an area under the curve (AUC) of 0.322, TWI did not prove a relevant parameter for differentiating between healthy and damaged cartilage (Fig. 3).

For 540 nm, however, the logistic regression model showed a good compatibility with an AUC of 0.878.

At a threshold of 540 nm > 0.74, a cartilage defect ICRS grade ≥ 3 could be detected with a sensitivity of 0.81 and a specificity of 0.81.

Discussion

This study aimed to investigate, whether HSI is able to detect areas of cartilage degeneration reliably by differentiating between healthy and damaged cartilage tissue.

In this prospective diagnostic study, the relative absorbance at 540 nm exerted the potential to differentiate between healthy or damaged cartilage with a sensitivity of 0.81 and a specificity of 0.81. This resembles a diagnostic accuracy close to that of magnetic resonance imaging. While the sensitivity of HSI is comparable to the sensitivity of MRI in detecting cartilage damage reported in the literature (0.72–a0.87), the specificity of HSI is lower than what is reported for MRI (0.86–a0.89)²⁷.

So far, spectral data for cartilage have mostly been acquired from animal cartilage^{23–26} or post-surgery samples of humans^{28–31}, analyzing the infrared spectrum. The changes in the absorption of several wavelengths in this spectrum were found to correlate with degenerative changes in collagen and other components of cartilage. The authors proposed that the amount of water in the cartilage would be a valuable parameter for the degree of cartilage degeneration. However, they were not able to analyze the tissue's water content, as the samples used were ex vivo and already dehydrated^{23,32}. Hence, some authors see a great potential in vivo spectral analysis of

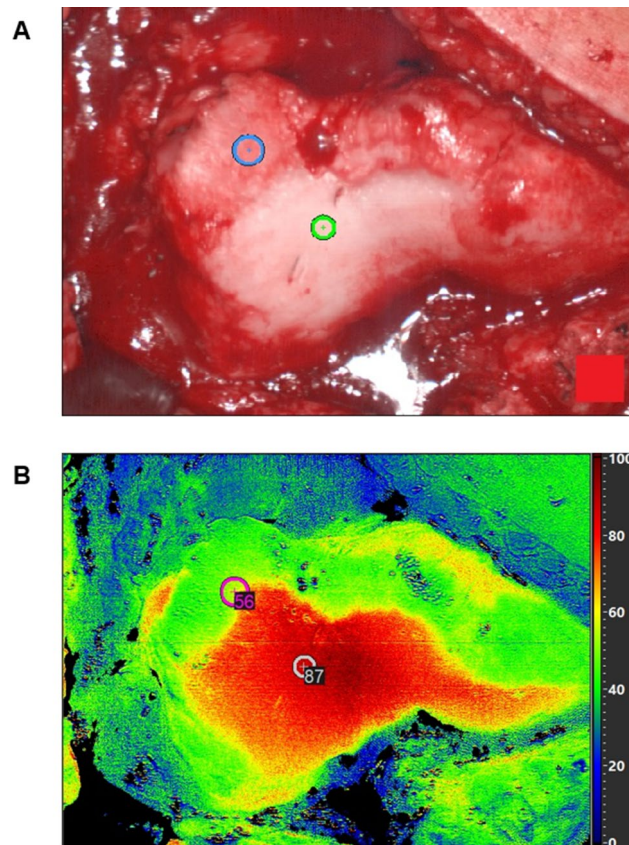


Figure 2. Example of a false color images for the TWI. **(A)** RGB image of the femoral trochlea joint surface. **(B)** Corresponding TWI image with ICRS grade 0 and ICRS grade 3 lesions marked.

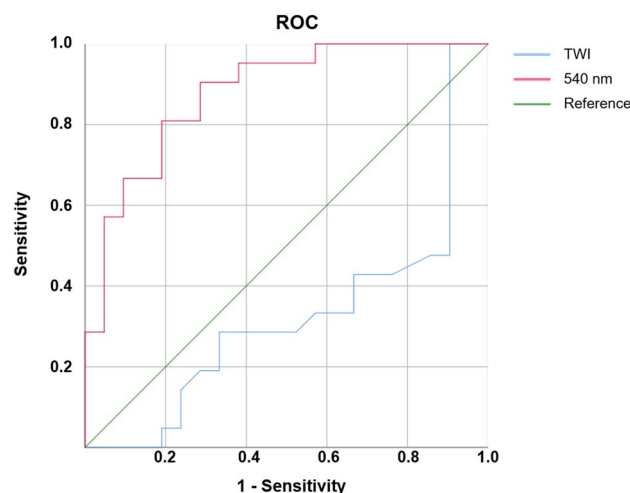


Figure 3. ROC analysis.

cartilage to detect degenerative changes early²³, and suggested that the NIR-spectrum would be useful³³. It was found that NIR-spectroscopy was a valuable method to distinguish low-grade lesions from healthy cartilage³⁴. Our findings are consistent with the previous studies, as the TWI value showed significant intraindividual differences between healthy and damaged cartilage. MRI also uses differences in water content to differentiate that⁵. However, the interindividual spread was too large to find a pragmatic TWI threshold value for clinical practice.

We found the relative absorbance at 540 nm to be a relevant parameter for the evaluation of cartilage tissue, using a threshold of >0.74 to detect cartilage lesions of ICRS grade ≥ 3 . This wavelength is within a spectral region

that shows peaks for oxygenated hemoglobin²². We suggest that in higher grade cartilage defects, HSI might detect a peak in that spectral region, because the cartilage gets thinner, allowing the bone tissue underneath to influence the spectral data.

HSI is a very recent technique and, thus, still limited in its clinical applications. One limitation is, that HSI can only be used on the tissue surface, as its penetration depth is a few millimetres only¹². For this study, the camera was used in open surgical approaches to the knee joint. For future applications, HSI needs to be combined and tested with arthroscopy or endoscopy to have a broader and more clinically relevant field of application. The results of this study are based on a sample size of 21 patients only. In order to confirm the preliminary findings of our data, studies with larger sample sizes are needed. This would allow for a more detailed differentiation of cartilage degeneration beyond the two extreme poles “healthy” and “damaged” and possibly more sophisticated information on the different “shades of gray” by the colourful spectra of Hyperspectral Imaging.

The ICRS grading system was used as the gold standard for determining the test accuracy of HSI. While the ICRS grading system is a well-validated standard, it is still just a tool to grade superficially visible defects of the cartilage. Future studies may add histopathology as a reference and the “gold standard” to be compared with the results of HSI.

In this cohort, 19 out of 21 patients were female and only cartilage of patients with knee surgery was included. This limits the external validity of our findings and different thresholds may apply for cartilage of the hip or shoulder, where the cartilage thickness is different. However, women are more often affected by cartilage degeneration than men and the most frequent localization of cartilage damage is the knee joint³⁵. Future studies with a larger sample size that include different joints may confirm the results of this pilot study.

In summary, our study clearly shows that HSI has a high potential for the evaluation of cartilage tissue. Compared to MRI, it has the advantage of being available intraoperatively with only seconds needed for the measurements. Thus, the surgical procedure is only slightly disturbed and prolonged. It is completely contactless and radiation-free. No external contrast-medium has to be applied to the patient—resulting in a highly effective and safe intraoperative diagnostic tool. Hopefully, it will be available through arthroscopy and endoscopy systems soon, as previously described by the LYSiS-system³⁶. This would allow immediate intraoperative decision support for the surgeon when assessing a cartilage lesion and potentially change the operative procedure by this innovative “real time” modality.

Conclusion

HSI can provide reliable parameters to differentiate between healthy and damaged cartilage. Therefore, it has the potential to serve as a valuable addition to arthroscopy, helping surgeons to identify critical lesions that are not visible with the naked eye.

Our data from a cohort of mainly elderly women suggest that the difference in absorbance at 540 nm is the best parameter to achieve accurate identification of damaged cartilage.

Data availability

All raw data can be provided by the corresponding author upon request.

Received: 16 July 2021; Accepted: 17 December 2021

Published online: 12 January 2022

References

- Litwic, A., Edwards, M. H., Dennison, E. M. & Cooper, C. Epidemiology and burden of osteoarthritis. *Br. Med. Bull.* **105**, 185–199 (2013).
- Hayashi, D., Roemer, F. W. & Guermazi, A. Imaging for osteoarthritis. *Ann. Phys. Rehabil. Med.* **59**(3), 161–169 (2016).
- Gersing, A. S., Schwaiger, B. J., Wörtler, K. & Jungmann, P. M. Dezidierte Knorpelbildgebung zur Detektion von Knorpelverletzungen und osteochondralen Läsionen. *Radiologe* **58**(5), 422–432 (2018).
- Berberat, J. E., Nissi, M. J., Jurvelin, J. S. & Nieminen, M. T. Assessment of interstitial water content of articular cartilage with T1 relaxation. *Magn. Reson. Imaging* **27**(5), 727–732 (2009).
- Recht, M. P., Goodwin, D. W., Winalski, C. S. & White, L. M. MRI of articular cartilage: Revisiting current status and future directions. *AJR Am. J. Roentgenol.* **185**(4), 899–914 (2005).
- Hofmann, G. O. *et al.* Detection and evaluation of initial cartilage pathology in man: A comparison between MRT, arthroscopy and near-infrared spectroscopy (NIR) in their relation to initial knee pain. *Pathophysiology* **17**(1), 1–8 (2010).
- Leschied, J. R., Smith, E. A., Baker, S., Khalatbari, S. & Aronovich, S. Contrast-enhanced MRI compared to direct joint visualization at arthroscopy in pediatric patients with suspected temporomandibular joint synovitis. *Pediatr. Radiol.* **49**(2), 196–202 (2019).
- Reed, M. E. *et al.* 3.0-Tesla MRI and arthroscopy for assessment of knee articular cartilage lesions. *Orthopedics* **36**(8), e1060–4 (2013).
- Engelhardt, L. V., von Schmitz, A. & Burian, B. *et al.* 3-Tesla-MRT vs. Arthroskopie bei der Diagnostik degenerativer Knorpelschäden des Kniegelenkes Erste klinische Ergebnisse. *Orthopade* **37**(9), 914, 916–22 (2008).
- Brittberg, M. & Winalski, C. S. Evaluation of cartilage injuries and repair. *J. Bone Joint Surg. Am.* **85**(2), 58–69 (2003).
- Bert, J. M. & Leverone, J. Histologic appearance of “pristine” articular cartilage in knees with unicompartmental osteoarthritis. *J. Knee Surg.* **20**(1), 15–19 (2007).
- Lu, G. & Fei, B. Medical hyperspectral imaging: A review. *J. Biomed. Opt.* **19**(1), 10901 (2014).
- Li, Q. *et al.* Review of spectral imaging technology in biomedical engineering: Achievements and challenges. *J. Biomed. Opt.* **18**(10), 100901 (2013).
- Roblyer, D. *et al.* Multispectral optical imaging device for in vivo detection of oral neoplasia. *J. Biomed. Opt.* **13**(2), 24019 (2008).
- Kiyotoki, S. *et al.* New method for detection of gastric cancer by hyperspectral imaging: A pilot study. *J. Biomed. Opt.* **18**(2), 26010 (2013).
- Beaulieu, R. J. *et al.* Automated diagnosis of colon cancer using hyperspectral sensing. *Int. J. Med. Robot.* **14**(3), e1897 (2018).
- Grambow, E. *et al.* Evaluation of peripheral artery disease with the TIVITA Tissue hyperspectral imaging camera system. *Clin. Hemorheol. Microcirc.* **73**(1), 3–17 (2019).

18. Chin, M. S. *et al.* Hyperspectral imaging provides early prediction of random axial flap necrosis in a preclinical model. *Plast. Reconstr. Surg.* **139**(6), 1285e–1290e (2017).
19. Calin, M. A. *et al.* Blood oxygenation monitoring using hyperspectral imaging after flap surgery. *Spectrosc. Lett.* **50**(3), 150–155 (2017).
20. Li, Q. *et al.* Automatic identification and quantitative morphometry of unstained spinal nerve using molecular hyperspectral imaging technology. *Neurochem. Int.* **61**(8), 1375–1384 (2012).
21. Zuzak, K. J. *et al.* Intraoperative bile duct visualization using near-infrared hyperspectral video imaging. *Am. J. Surg.* **195**(4), 491–497 (2008).
22. Holmer, A., Marotz, J., Wahl, P., Dau, M. & Kämmerer, P. W. Hyperspectral imaging in perfusion and wound diagnostics—methods and algorithms for the determination of tissue parameters. *Biomed. Tech. (Berl)* **63**(5), 547–556 (2018).
23. Bi, X., Yang, X., Bostrom, M. P. G. & Camacho, N. P. Fourier transform infrared imaging spectroscopy investigations in the pathogenesis and repair of cartilage. *Biochim. Biophys. Acta* **1758**(7), 934–941 (2006).
24. Kiviranta, P. *et al.* Collagen network primarily controls Poisson's ratio of bovine articular cartilage in compression. *J. Orthop. Res.* **24**(4), 690–699 (2006).
25. West, P. A., Torzilli, P. A., Chen, C., Lin, P. & Camacho, N. P. Fourier transform infrared imaging spectroscopy analysis of collagenase-induced cartilage degradation. *J. Biomed. Opt.* **10**(1), 14015 (2005).
26. Boskey, A. & Pleshko Camacho, N. FT-IR imaging of native and tissue-engineered bone and cartilage. *Biomaterials* **28**(15), 2465–2478 (2007).
27. Harris, J. D. *et al.* Sensitivity of magnetic resonance imaging for detection of patellofemoral articular cartilage defects. *Arthroscopy* **28**(11), 1728–1737 (2012).
28. Bi, X., Li, G., Doty, S. B. & Camacho, N. P. A novel method for determination of collagen orientation in cartilage by Fourier transform infrared imaging spectroscopy (FT-IRIS). *Osteoarthr. Cartil.* **13**(12), 1050–1058 (2005).
29. Korhonen, R. K. *et al.* Collagen network of articular cartilage modulates fluid flow and mechanical stresses in chondrocyte. *Biomech. Model. Mechanobiol.* **5**(2–3), 150–159 (2006).
30. David-Vaudey, E. *et al.* Fourier Transform Infrared Imaging of focal lesions in human osteoarthritic cartilage. *Eur. Cell. Mater.* **10**, 51–60; discussion 60 (2005).
31. West, P. A. *et al.* Fourier transform infrared spectral analysis of degenerative cartilage: An infrared fiber optic probe and imaging study. *Appl. Spectrosc.* **58**(4), 376–381 (2004).
32. Camacho, N. P., West, P., Torzilli, P. A. & Mendelsohn, R. FTIR microscopic imaging of collagen and proteoglycan in bovine cartilage. *Biopolymers* **62**(1), 1–8 (2001).
33. Padalkar, M. V., Spencer, R. G. & Pleshko, N. Near infrared spectroscopic evaluation of water in hyaline cartilage. *Ann. Biomed. Eng.* **41**(11), 2426–2436 (2013).
34. Spahn, G., Plettenberg, H., Kahl, E., Klinger, H. M., Mückley, T. & Hofmann, G. O. Near-infrared (NIR) spectroscopy. A new method for arthroscopic evaluation of low grade degenerated cartilage lesions. Results of a pilot study. *BMC Musculoskelet. Disord.* **8**, 47 (2007).
35. Srikanth, V. K. *et al.* A meta-analysis of sex differences prevalence, incidence and severity of osteoarthritis. *Osteoarthr. Cartil.* **13**(9), 769–781 (2005).
36. Köhler, H. *et al.* Laparoscopic system for simultaneous high-resolution video and rapid hyperspectral imaging in the visible and near-infrared spectral range. *J. Biomed. Opt.* **25**(8), 086004 (2020).

Author contributions

M.K. participated in designing the study, data acquisition and data analysis and drafted part of the manuscript. H.K. participated data acquisition and data analysis and revised the manuscript. J.T., A.R. and P.H. participated in designing the study, patient recruiting and data acquisition and revised the manuscript. I.G. participated in designing the study and data analysis and revised the manuscript. G.O. had the idea for the study, participated in designing the study, patient recruiting, data acquisition and data analysis and drafted part of the manuscript.

Funding

Open Access funding enabled and organized by Projekt DEAL. No funding was received for the measurements and/or preparation of this manuscript.

Competing interests

The hyperspectral camera used for the measurements in this publication was developed by Diaspective Vision GmbH. HK was an employee of this company. All other authors have no conflicts of interests.

Additional information

Correspondence and requests for materials should be addressed to G.O.

Reprints and permissions information is available at www.nature.com/reprints.

Publisher's note Springer Nature remains neutral with regard to jurisdictional claims in published maps and institutional affiliations.



Open Access This article is licensed under a Creative Commons Attribution 4.0 International License, which permits use, sharing, adaptation, distribution and reproduction in any medium or format, as long as you give appropriate credit to the original author(s) and the source, provide a link to the Creative Commons licence, and indicate if changes were made. The images or other third party material in this article are included in the article's Creative Commons licence, unless indicated otherwise in a credit line to the material. If material is not included in the article's Creative Commons licence and your intended use is not permitted by statutory regulation or exceeds the permitted use, you will need to obtain permission directly from the copyright holder. To view a copy of this licence, visit <http://creativecommons.org/licenses/by/4.0/>.

© The Author(s) 2022